Free-energy measuring nanopore device

Momčilo Gavrilov,[1,*] Jinghang Zhang,[2] Olivia Yang,[1] and Taekjip Ha[1,2]
[1]*Johns Hopkins University School of Medicine, Department of Biophysics and Biophysical Chemistry, 725 N. Wolfe Street, Baltimore, Maryland 21205, USA*
[2]*Johns Hopkins University, Department of Biomedical Engineering, 720 Rutland Avenue, Baltimore, Maryland 21205, USA*

(Received 18 May 2023; revised 15 October 2023; accepted 5 December 2023; published 9 February 2024)

Free energies (FEs) in molecular sciences can be used to quantify the stability of folded molecules. In this article, we introduce nanopores for measuring FEs. We pull DNA hairpin-forming molecules through a nanopore, measure work, and estimate the FE change in the slow limit, and with the Jarzynski fluctuation theorem (FT) at fast pulling times. We also pull our molecule with optical tweezers, compare it to nanopores, and explore how sampling single molecules from equilibrium or a folded ensemble affects the FE estimate via the FT. The nanopore experiment helps us address and overcome the conceptual problem of equilibrium sampling in single-molecule pulling experiments. Only when molecules are sampled from an equilibrium ensemble do nanopore and tweezer FE estimates mutually agree. We demonstrate that nanopores are very useful tools for comparing FEs of two molecules at finite times and we propose future applications.

DOI: 10.1103/PhysRevE.109.024404

I. INTRODUCTION

The behavior of many chemical and biological systems at the molecular level is often described by their free-energy (FE) diagrams [1–3]. Single-molecule techniques such as optical, magnetic, or acoustic tweezers and atomic force microscopy (AFM) provide a direct control of individual molecules and can estimate the stochastic work [3–12], while fluctuation theorems (FTs) provide a method for extracting FE values from stochastic work measurements [2,13–16]. Led by earlier experimental tests of FTs in biophysics [5–9], we introduce a FE measuring nanopore device to complement existing single-molecule manipulation tools and to address and overcome related practical and fundamental challenges, including sampling the equilibrium ensemble, corrections to bulky probes and handles, extending the range of pulling rates, and applying a stochastic instead of mechanical work definition [13,17].

We first enable a nanopore device for high-accuracy work and FE measurements in unfolding experiments with sub-kT precision and apply it to a 10–base pair (bp) DNA hairpin. Then we compare nanopore and optical tweezers estimates and find the following:

(1) When the work distribution is based on pulling molecules from the equilibrium ensemble as required by FTs [2,13], tweezers and nanopore experiments yield similar FE values of 5.5 ± 0.4 kT and 5.25 ± 0.06 kT, respectively, for our 10-bp DNA hairpin. These values are further consistent with the FE estimate based on the equilibrium measurement $\approx$5.5 kT and measurement in the slow limit, 5.7 ± 0.6 kT.

(2) When the work distribution is based on pulling molecules from the folded ensemble, tweezers and nanopore FEs are overestimated and they mutually disagree.

Our experiments and discussion help make a clear distinction between folded and equilibrium ensembles as is essential for the correct FE estimate via FTs and the interpretation of FTs [2,13,16]. As long as molecules are drawn from an equilibrium ensemble, moderate corrections applied to measured work values have a negligible impact on the FE estimate, in stark contrast to the pronounced influence of such corrections on the mean work. This behavior we attribute to the negative exponential averaging inherent in the FT. We also propose a line of problems in biophysics to address with nanopores.

A. Molecular system

We pull a 10-bp DNA hairpin molecule. The hairpin sequence is GCT CTG TTG C TCT CTC G CAA CAG AGC followed by poly-A(A_{28}) and diluted in 500 mM KCl buffer at 22 °C. The equilibrium ensemble of individual hairpin molecules in a test tube is schematically illustrated in Fig. 1(a). This ensemble predominately consists of folded molecules where the underlined nucleotides are hybridized or base paired through hydrogen or H bonds to form a DNA hairpin [18]. Folded molecules cannot pass through a narrow pore until H bonds are dissociated and the molecule unfolded [Fig. 1(b)]. A small fraction ($\rho \approx 0.4\%$) of molecules in the equilibrium ensemble are unfolded with dissociated H bonds and they can pass through the pore without the need to unfold first. Each molecule in equilibrium [Fig. 1(a)] can spontaneously unfold and fold due to thermal fluctuations, but ρ of the thermodynamic ensemble in the test tube is constant [1,19]. The fraction ρ depends on the buffer condition, salt concentration, pH, the length of the duplex, sequence, length of the loop, temperature, etc. [20]. A nanopore method can

*Author to whom correspondence should be addressed: momcilo.gavrilov@gmail.com, he/him/his

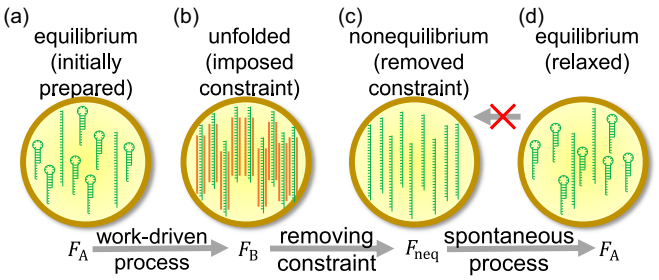

FIG. 1. DNA hairpins in buffer solution. (a) Equilibrium ensemble consists of folded molecules, while a fraction ρ is unfolded. (b) Unfolding by imposing a spatial constraint requires work. (c) Removing nanopore constraint. (d) Unfolded hairpins spontaneously equilibrate after sufficient time.

identify unfolded and folded molecules and count them to estimate ρ.

B. Definition

We estimate the Helmholtz free-energy (HFE) difference per molecule, $\Delta F = F_B - F_A$, between the unfolded [Fig. 1(b) or 1(c), F_B] and equilibrium [Fig. 1(a), F_A] ensemble of DNA hairpins in an experiment where we pull and unfold molecules one by one through a protein α-hemolysin (αHL) pore. We adapt a textbook definition of HFE difference [1]: The HFE difference (ΔF) between the unfolded [Fig. 1(b)] and equilibrium [Fig. 1(a)] ensemble of DNA hairpins contained in a constant volume is the maximal or beneficial work that unfolded hairpins may perform as they reach equilibrium under the constant temperature. Unfolded molecules in Fig. 1(b) can perform work after we remove the constraint keeping them unfolded [Fig. 1(c)]. A more common quantity used to describe the stability of a molecule is the FE parameter $\Delta G^o_T = -\mathrm{kT} \ln K$, where the equilibrium constant $K = [(1-\rho)/\rho]$ is defined as the ratio of folded and unfolded fractions in equilibrium. The quantity ΔF is defined through the beneficial work, while ΔG^o_T is defined through fractions of molecules in equilibrium; nevertheless, we will show that numerical values for ΔF and ΔG^o_T are similar for our molecule. Nanopores were previously utilized to determine rates and activation energies of DNA translocation through the pore [18,21,22], but to the best of our knowledge nanopores were not utilized to measure work and FEs ΔF or ΔG^o_T with FTs.

II. PROBLEMS, FEATURES, AND PROGRESS

Optical tweezers and AFM can measure various thermodynamic properties of single molecules [2], including work, heat, FE change, and entropy production [5–9]. Our nanopore approach is inspired by previous tweezers and AFM studies, but it also offers an alternative for studying molecules with several important features:

Feature 1. The nanopore method samples and pulls an equilibrium ensemble of molecules, containing also a small fraction ρ of unfolded molecules [Fig. 1(a)] and can test how a sampling difference between the folded and equilibrium ensemble affects the FE estimate. Direct detection of a small fraction of unfolded molecules in equilibrium remains challenging for tweezers and AFM, and consequently tweezers and AFM only sample folded molecules.

Feature 2. The nanopore method removes the need for any correction of measured work and FE values because it samples free-diffusing molecules from solution [Fig. 1(a)], without ligated adapters or probes. Measured nanopore work values are used to estimate the reported change in the FE without corrections. Optical tweezers and AFM require tethering of a molecule to the surface of a slide, micropipette, or bead, and additional modifications, adapters, or handles, and many tweezers and AFM experiments introduce various corrections into the analysis to account for beads, handles, and probes.

Feature 3. The nanopore method uses electric forces for pulling molecules. Nanopores can operate with pulling powers, in our case spanning over three orders of magnitude. At the highest power, a nanopore can pull a molecule within 2 ms, while minimal pulling times of tweezers and AFM are at the order of 100 ms.

Feature 4. This feature is related to the analysis, and is not a hardware feature. The nanopore method obtains the stochastic work directly from the time-dependent electric potential [13,17] by integrating the pulling power in time. Several tweezers and AFM studies used the mechanical work definition [5–7,9] as the integral of force versus displacement. The mechanical work definition does not generally lead to the FE estimate via FT [13], and the correct work definition has been a subject of other debates [17,23,24].

III. NANOPORE SETUP AND MEASUREMENT

The nanopore setup [Fig. 2(a)] consists of two chambers at positions $x = 1$ and $x = 0$ connected by an αHL pore [18,21,26–29]. An electrode in each chamber is connected to an external power supply (Axon Axopatch 200B) capable of recording picoampere currents through the pore and controlling the applied voltage with a custom LABVIEW code at 0.2 MHz. When a potential difference or voltage $V(t)$ is applied to the electrodes [Fig. 2(a), top], the electric potential $\phi(x,t)$ in each chamber is nearly "flat," while the major potential drop occurs within the pore [25]. The potential drop along the 10-nm-long nanopore has a strong gradient; hence, it generates a pulling force on any charged molecule in the pore. We keep the right-hand electrode at 0 mV, while the left-hand electrode voltage $V(t)$ can be set between 0 and 200 mV and it serves as our control parameter to set the potential $\phi(x,t)$. DNA hairpins are negatively charged in our buffer solution because of their phosphate backbone. We followed a previously described protocol to measure the effective charge of our molecules in a nanopore device [18,28,29] and determined the effective charge of $q = 2.06 \pm 0.08e$ or -0.080 ± 0.003 kT/mV in our buffer solution condition (500 mM KCl, 50 mM HEPES pH 9.0, 22 °C; see the Appendix). With the known q, we can estimate the potential energy in kT units anywhere in the chamber as $U(x,t) = q\phi(x,t)$.

A. Pulling experiment

We pipette in an equilibrium ensemble of molecules to the left chamber and start the experiment while waiting for a molecule to diffuse into the nanopore. When a molecule

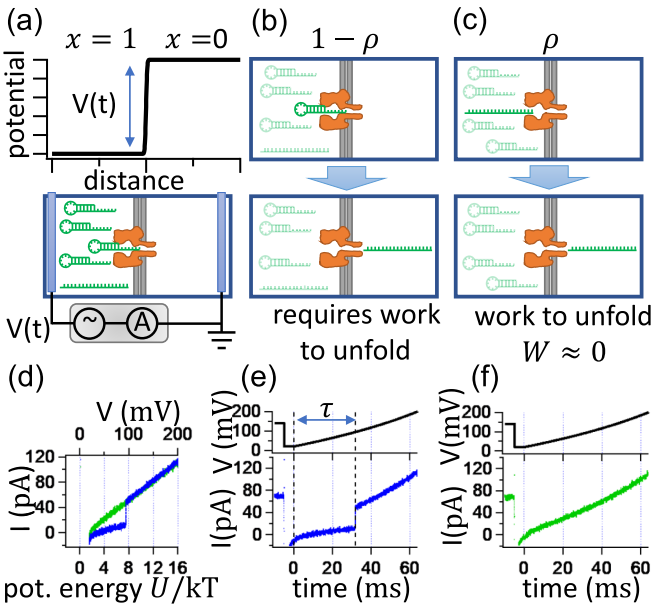

FIG. 2. Nanopore pulling method. (a) Nanopore setup and the potential energy. The potential drop occurs in the ≈1-nm pore, while the potential in chambers is nearly "flat" [25]. (b) Folded molecules require work of several kT to dissociate the duplex. (c) Unfolded molecules quickly pass through the pore, $W \approx 0$. (d) Electric current vs voltage and potential energy for molecules starting folded (blue) and unfolded (green). (e) Current and voltage time trace for an initially folded molecule. (f) Current and voltage time trace for an initially unfolded molecule.

diffuses into the pore we start to ramp up the voltage to $V_{\max} = 200\,\text{mV}$ to pull the molecule through. An unfolded DNA molecule quickly translocates through the pore [Fig. 2(c)]. A folded molecule [Fig. 2(b)] initially blocks the pore and it requires work of several kT to dissociate H bonds, unfold, and then translocate through the pore. The pulling duration or the time to ramp the voltage up to 200 mV in Fig. 2(e) is set to $t_0 = 64$ ms, and the unfolding of the ith molecule shown occurred at $\tau_i \approx 32$ ms or when the voltage reached $V(\tau_i) \approx 100$ mV. After dissociating H bonds and unfolding, a molecule quickly ($\varepsilon_t \ll t_0$) translocates through the pore into the $x = 0$ or the right-hand-side chamber, detected as a sudden discontinuous increase in the electric current.

In the next section, we show that the work to unfold the ith molecule as we gradually increase the potential difference can be expressed as $W_i = qV(\tau_i)$, where q is the effective charge and $V(\tau_i)$ is the voltage reached at the moment of unfolding, τ_i. For the example signal in Fig. 2(e) this leads to the work value of $W_i = qV(\tau_i) \approx 0.080\,\text{kT/mV} \times 100\,\text{mV} = 8$ kT. For every other repetition of the measurement, a molecule unfolds at different voltage, $V(\tau_i)$, leading to the stochasticity in work values represented with the work distribution $p(W)$ in Fig. 3(a).

B. Work definition

For a time-dependent change of a potential in a protocol of duration t_0, the work W_i to change the energy of the ith molecule in the chamber can be defined as

$$W_i = \int_0^{t_0} \frac{\partial U(x,t)}{\partial t}\bigg|_{x_i(t)} dt = \int_0^{t_0} P(t)dt, \qquad (1)$$

where $x_i(t)$ is the position of the hairpin loop of the ith molecules. The quantity $P(t)$ is the power in kT/ms units used to pull the molecule. This definition of work is common in

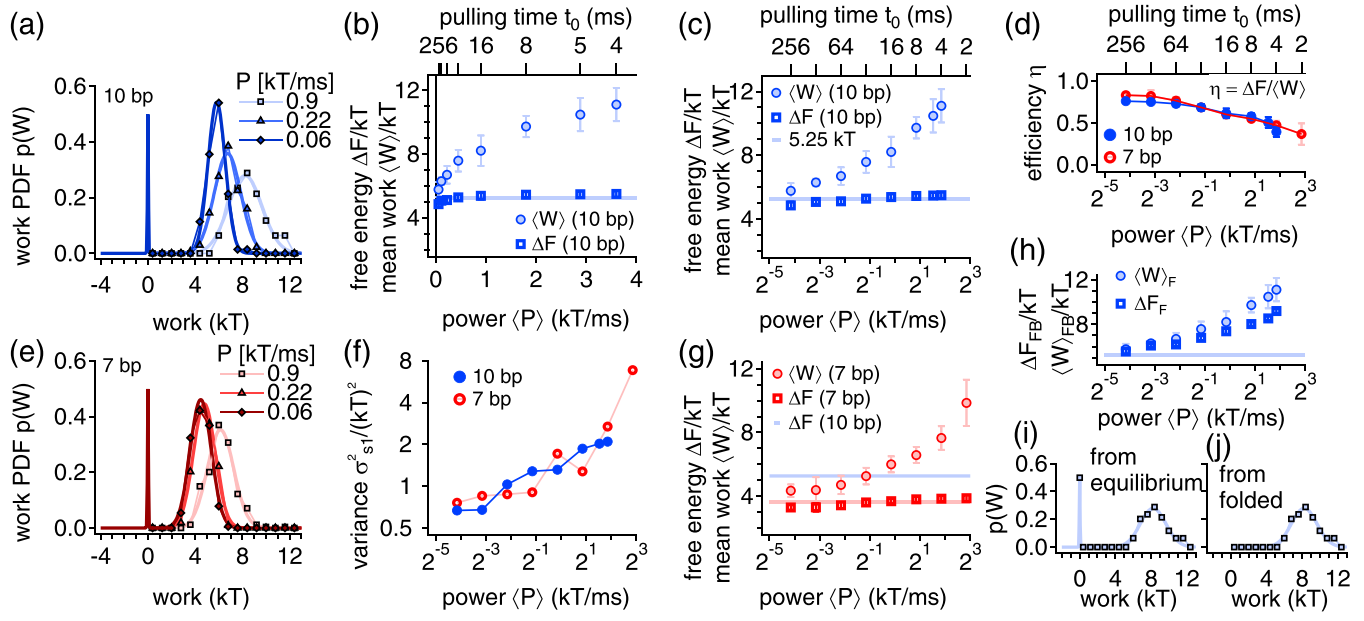

FIG. 3. Work and HFE difference estimate. (a) Work probability density functions (PDFs) for 10-bp hairpin. (b) The average work and the HFE difference. (c) linear-log plot of graph in (b). (d) The unfolding efficiency η. (e) Work PDF for 7-bp sequence. (f) Work variance for molecules starting folded. (g) The 7-bp hairpin has lower ΔF than the 10-bp hairpin. (h) The average work and the HFE difference for molecules starting folded. [(i) and (j)] Work distributions based on pulling molecules from equilibrium and folded ensembles. Solid horizontal lines in (b), (c), (g), and (h) show averaged ΔF values for 10-bp (5.25 kT, blue) and 7-bp (3.62 kT, red) hairpins.

stochastic thermodynamics and many other discussions about the microscopic foundations of macroscopic thermodynamics [2,13,30–32] and it is recommended in the context of the FT [17]. Unlike the force-displacement work definition, $W_0 = \int \vec{f} \cdot d\vec{r}$, Eq. (1) only requires knowing the change in the potential energy evaluated at a molecule's position.

1. Work integral for initially folded molecules

To estimate the work value W_i from the recorded signal in Fig. 2(e), we split the integral in Eq. (1) into three characteristic times $\int_0^{t_0} = \int_0^{\tau_i} + \underbrace{\int_{\tau_i}^{\tau_i+\varepsilon_t}}_{\approx 0} + \underbrace{\int_{\tau_i+\varepsilon_t}^{t_0}}_{=0}$ and obtain three values separately. From time zero to τ_i, the hairpin is folded and it blocks the pore. At time τ_i, H bonds dissociate and molecules quickly translocate through the pore in a very short time ε_t. After translocation, the pore remains open as we continue ramping the voltage up to $V_{\max} = 200$ mV to finish the cycle. The third integral vanishes, because after unfolding, a molecule enters the chamber where the potential is static, $U(0,t) = 0$. The second term is negligible because a molecule translocates through the pore much faster than we change the potential, $\varepsilon_t \ll t_0$. Only the first term determines the work to unfold as $W_i \approx \int_0^{\tau_i} P(t)dt = qV(\tau_i)$, and it can be determined by controlling the power $P(t)$ via voltage and measuring the unfolding time τ_i. We use a linear ramp function, where the voltage is controlled as $V(t) = V_{\max}(t/t_0)$; hence, the potential energy in the left-hand ($x = 1$) chamber is $U(1,t) = qV_{\max}(t/t_0)$ and the pulling power is constant: $P = \partial U/\partial t|_x = \partial(qV_{\max}t/t_0)/\partial t|_x = qV_{\max}/t_0$.

Current versus potential energy in Fig. 2(d) shows work as a value of the potential energy at which the current discontinuously increases. For each repetition of the pulling experiment, a molecule unfolds at different time τ_i and this leads to a different stochastic work value W_i. By repeating the pulling experiment several hundred times, we can reconstruct the work distribution by binning and normalizing the histogram [Fig. 3(a)]. It is noteworthy that the electric current value in picoamperes is not directly used to calculate power or work needed to unfold one single molecule. The electric current is rather used to determine the unfolding time τ_i.

2. Work integral for initially unfolded molecules

Not all detected molecules are initially folded and behave as described in Fig. 2(b). A small fraction ρ of detected molecules is initially unfolded with dissociated H bonds [Fig. 2(c)]. Unfolded molecules also diffuse into the nanopore and trigger recording, but they quickly translocate through in less than 0.5 ms, leaving the pore open [Figs. 2(c) and 2(f)]. Unfolded DNA hairpins behave similar to a linear DNA sequence, i.e., $(A)_{90}$, and translocate through in less than 0.5 ms [18]. We estimate the unfolded fraction by dividing the number of unfolded molecules by the total number of molecules and obtain $\rho = \rho_{10} = 18/4056 \approx 0.4\%$ for the 10-bp hairpin and $\rho_7 = 85/4175 \approx 2\%$ for the 7-bp hairpin. Since the fraction ρ is already unfolded, nearly zero work is spent on dissociating H bonds and unfolding and we assign zero work $W_i = 0$ for each unfolded molecule entering the pore.

3. Work distributions

After pulling a few hundred molecules at fixed pulling duration $t_0 = 64$ ms (or power $P \sim 1/t_0$) and measuring work, we reconstruct the work probability density functions (PDFs) or work distribution [Fig. 3(a)]. The pulling procedure is repeated at other pulling times (4, 5, 8, 16, 32, 64, 128, and 256 ms) and for each pulling time we reconstructed a PDF. Reconstructed work PDFs have two peaks because of two fractions in equilibrium [Fig. 3(a)]. The unfolded fraction ρ contributes to a peak at zero work, $W = 0$, with the area under of $\rho = 0.4\%$. Broad peaks in Fig. 3(a) correspond to the folded fraction $(1 - \rho)$ and those peaks are nearly Gaussian.

C. Result

Figures 3(b) and 3(c) show the mean work obtained from PDFs in Fig. 3(a) versus P and t_0 with more work required to unfold at higher powers or faster pulling times. From the second law and the Clausius inequality, $\Delta F \leqslant \langle W \rangle$, the HFE difference is smaller than the mean work [1,19], at the lowest P, $\Delta F_{10\text{bp}} \leqslant 5.7 \pm 0.6$ kT.

The Jarzynski FT estimates ΔF no matter how far from equilibrium the process is carried out [5,13]. ΔF is linked to the measured work W via the expression

$$\frac{\Delta F}{\text{kT}} = -\ln\left\langle \exp\left(-\frac{W}{\text{kT}}\right)\right\rangle, \tag{2}$$

where $\langle\cdot\rangle$ indicates the exponential averaging. We estimate ΔF with the FT and display it in Figs. 3(b) and 3(c). The HFE estimates via Eq. (2) are practically independent of the pulling power and yield to $\Delta F_{10\text{bp}} = 5.25 \pm 0.06$ kT when averaged over all powers, indicated with the horizontal line in Figs. 3(b) and 3(c) (square markers). This value is close to the mean work of 5.7 ± 0.6 kT at the lowest power but is much below the mean work of 11.1 ± 0.1 kT at the highest power.

Overall, for an equilibrium ensemble of molecules, we recovered the HFE difference from work measurements in a range of pulling powers spanning over three orders of magnitude. We also followed several good practices for better FE estimates [33–35], suggesting to transform the work PDF in Fig. 3(a), rather than substituting individual work values into Eq. (2). Equation (2) provides the exact ΔF value only for an infinite number of error-free measurements, while for a finite number of nonideal measurements where the work PDF for initially folded molecules can be approximated as Gaussian, we derive a more robust expression [Eq. (8)] to minimize the bias in the FE estimate.

The pivotal requirement for applying Eq. (2) is to ensure that molecules are sampled from an equilibrium ensemble, encompassing contributions from both initially folded and initially unfolded molecules in the work PDF, as illustrated in Fig. 3(i). Failing to include the ρ fraction of initially unfolded molecules and the corresponding peak on the left-hand side [Fig. 3(i)] can result in an inaccurate estimation of FE. In fact, omitting the left-hand-side peak in Fig. 3(j) leads to inconclusive FE estimates that become strongly dependent on the loading rate, as demonstrated in Fig. 3(h) (square markers). To prevent such nonphysical outcomes, it is imperative to incorporate work measurements from both initially folded and unfolded molecules in the analysis.

We also repeated nanopore measurements with a 7-bp sequence GTC GAA C TTTT G TTC GAC followed by poly-A(A_{27}), where we expect the FE to be lower than for the 10-bp sequence. We show work PDFs for the 7-bp sequence in Fig. 3(e), show the mean work and HFE difference in Fig. 3(g), and find the FE of $\Delta F_{7\text{bp}} = 3.62 \pm 0.06$ kT, lower than for the 10-bp sequence, as expected because the 7-bp DNA hairpin has overall fewer H bonds than the 10-bp hairpin.

The unfolding efficiency $\eta(P)$ was estimated as the ratio of the HFE difference ΔF and the average work $\langle W \rangle|_P$ spent at each power, $\eta(P) = \Delta F / \langle W \rangle|_P \leqslant 1$ [Fig. 3(d)]. The pulling efficiency varies from 0.83 at the lowest power to 0.38 at the highest power. This efficiency was estimated for the pulling protocol where the voltage linearly increases in time. The nanopore method can also implement many different pulling voltage protocols to explore the optimization, minimize the dissipation at the fixed t_0 [10], and even explore protocols shaping distinctly non-Gaussian work distributions.

IV. OPTICAL TWEEZERS EXPERIMENT

To assess the quality of the nanopore method and better understand its advantages, we compare it to a more established optical-tweezers experiment applied to our 10-bp hairpin in the same buffer and temperature. The tweezers experiment also helps us quantify, explore, and explain how the difference between sampling molecules from folded or equilibrium ensembles affects the FE estimate via Eq. (2). We used a commercial instrument from Lumicks model C-trap and ligated our 10-bp hairpin between two beads of 0.8 μm diameter using double-stranded DNA tethers of 1500 and 1700 bp [Fig. 4(g)] [36]. In the pulling experiment, the left-hand tether is fixed, while the position of the right-hand laser focus $\lambda(t)$ serves as the control parameter and moves from 6.0 to 6.5 μm over 12 s [Fig. 4(a)]. With the fast position-sensitive detector (PSD), tweezers measure the displacement of the bead from the laser focus, ΔX [Fig. 4(b)]. The recorded position ΔX in Fig. 4(b) fluctuates around 0 nm from 0 to 7 s, because initially DNA tethers are relaxed [Fig. 4(g)]. At about 7 s, the bead is displaced farther from the center of the trap and ΔX gradually increases from 7 to 10 s. At about 10 s, we observed a discontinuous drop in the bead position ΔX of about 4 nm, a consequence of abrupt one-step unfolding of the DNA hairpin and the dissociation of H bonds between the duplex. The change in ΔX of about 4 nm is a consequence of increased length of the unfolded hairpin and relaxation of attached handles. The bead-position measurement ΔX is further used to calculate the force magnitude $f = \kappa \Delta X$, where the trap stiffness of $\kappa = 0.31 \pm 0.01$ pN/nm was obtained in the automatic calibration of the C-trap instrument. We superimposed several different force traces versus the laser position λ in Fig. 4(c) showing that for each repetition, the molecule unfolds at a different force value. The force plot in Fig. 4(c) is a common way to represent tweezers data.

A. Work estimate

To determine the change in FE using the optical tweezers experiment and facilitate a meaningful comparison with the nanopore results, our first step is to estimate the work to unfold a molecule in units of kT for each recorded trajectory. We then apply Eq. (2) for our analysis. In the field of biophysics, a commonly used work definition integrates force and provides mechanical work, denoted as W_0 [5–7,9,10]. However, it is crucial to note that the derivation of the FT in Eq. (2) did not rely on the use of mechanical work, and it is not recommended or expected to yield the correct FE value in this context [2,2,13,17,23,24].

Instead, Eq. (1) defines work as the integration of dissipated power over time, expressed as $dW = Pdt$, which we

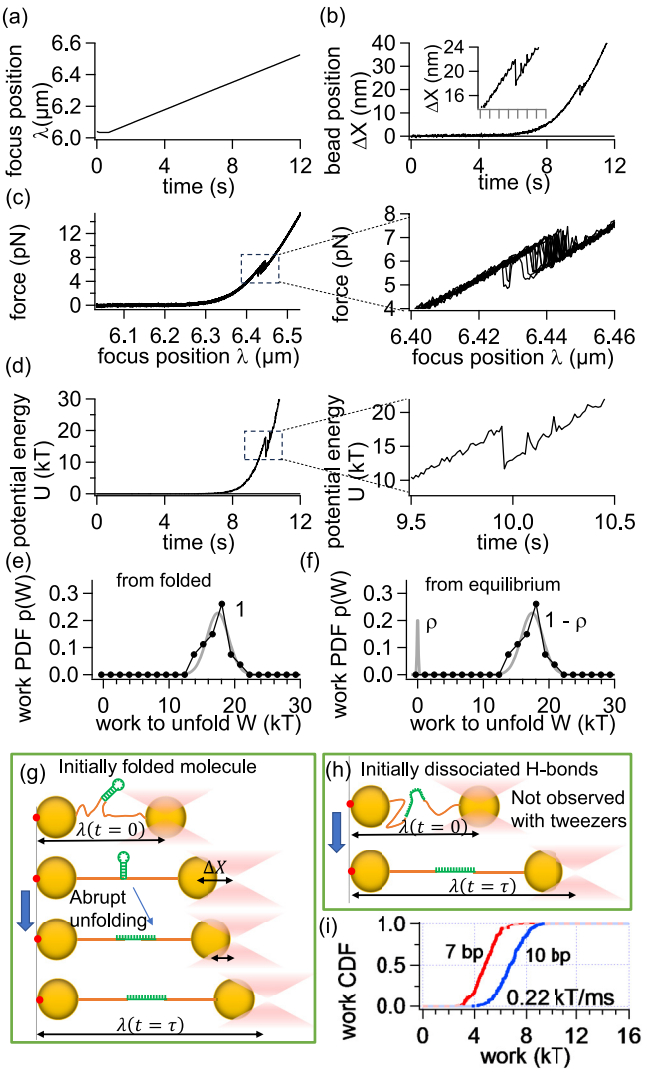

FIG. 4. Tweezers experiment. (a) Laser-focus position λ moves from 0 to 6.5 μm over 12 s. (b) Measured bead position relative to the laser focus recorded on the position-sensitive detector (PSD). (c) Force vs laser position λ for several traces. (d) Potential energy calculated from the bead position trace in (a). (e) Work PDF reconstructed from pulling molecules from the folded ensemble. (f) Work PDF reconstructed from pulling molecules from the equilibrium ensemble. [(g) and (h)] Illustration of tweezers pulling experiment for initially folded and unfolded molecules, respectively. (i) Comparing nanopore work cumulative distribution functions (CDFs) for 10- and 7-bp DNA hairpins at fixed pulling rate; 7-bp hairpin requires about 2 kT less work to unfold than the 10-bp hairpin.

refer to as the stochastic work definition. It is essential to utilize the stochastic work definition in the context of Eq. (2) to obtain the correct ΔF value, as established in previous studies [2,13,17,23,24]. This work definition has been employed in both experimental investigations exploring fundamental questions in statistical mechanics [31,32,37–47] and certain biophysics studies [8]. In the following section, we provide more detailed insights into the stochastic work integral as described in Eq. (1). Additionally, in the Appendix, we offer a comprehensive comparison between the stochastic and mechanical work definitions within the context of tweezers data.

1. Work integral

We integrate the stochastic work defined in Eq. (1) in three steps. First, we calculate the potential energy in kT units $U(\Delta X) = \frac{1}{2}\kappa(\Delta X)^2$ in the harmonic trap from the recorded trajectory in Fig. 4(b) and show how the potential energy $U(\Delta X)$ evolves in time in Fig. 4(d). Figure 4(d) shows a discontinuous drop in the potential energy from 18 kT at about 10 s, as a consequence of abrupt unfolding. Second, we calculate the dissipated power in the pulling experiment, $P = \frac{\partial U(x,t)}{\partial t}|_x$, as the slope from the potential energy in Fig. 4(d). The dissipated power versus time is shown in Fig. 5(a). Third, we integrate the dissipated power over time until the molecule unfolds at about 10 s in Fig. 5(b) and obtain the work value of ≈18 kT from the integral.

For every repetition of the tweezers pulling experiment [Fig. 4(b)], the molecule unfolds at different time, leading to the stochasticity in work values. The tweezers experiment also involves other accompanying processes, such as stretching tethers and unfolded single-stranded DNA, dragging beads through the fluid, etc. The work value of 18 kT obtained from the trace in Fig. 4(b) also includes the dissipation due to other accompanying processes. We applied no correction to obtain the work value of 18 kT. We collected work values from 48 trajectories, and through binning the work values in a histogram and normalizing, we obtain the work PDF in Fig. 4(e).

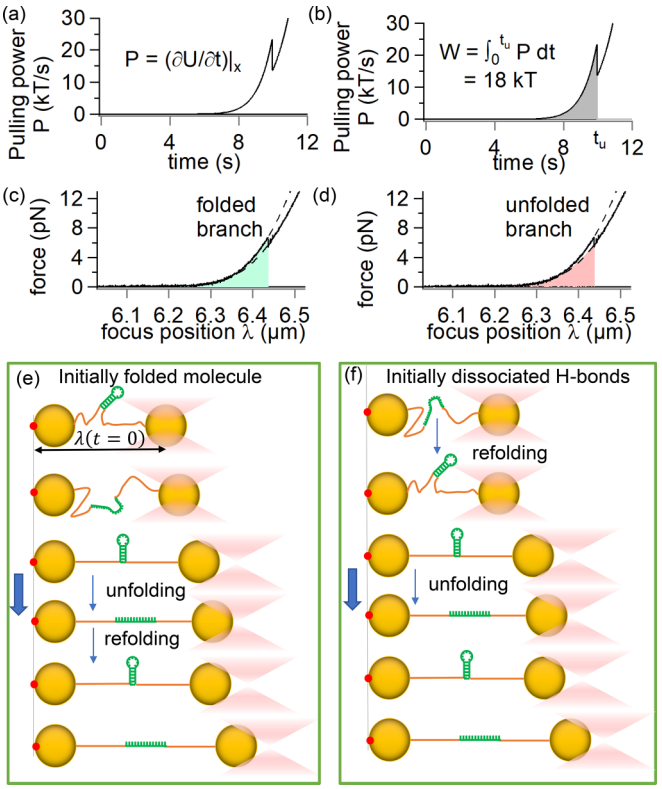

FIG. 5. Calculating work in the tweezers experiment. (a) The pulling power is estimated from the change in the potential energy [Fig. 4(d)] in time. (b) The work to unfold integrates power until a molecule unfolds at about 10 s and leads to the work value of ≈18 kT. (c) Force vs laser position λ is used to estimate the mechanical work. The top branch corresponds to folded molecules and the integrated area is 358.1 kT. (d) The area under the bottom or unfolded branch is 298.7 kT. This value is usually associated with the work to stretch elastic handles. (e) Pulling initially folded molecules in the slow limit may result in multiple fluctuations between the folded and unfolded conformations. (f) Pulling initially unfolded molecules in the slow limit may result in multiple fluctuations between the folded and unfolded conformations.

V. DISCUSSION AND DERIVATION

For the work PDF obtained in the tweezers experiment [Fig. 4(e)], we find the mean $\langle W_{\rm twz}\rangle = 17.2 \pm 0.4$ kT, and applying Eq. (2) to the work PDF in Fig. 4(e) outputs the ΔF value of ≈15.6 kT. The value of ≈15.6 kT obtained in the tweezers experiment is more than three times higher than the FE value of 5.25 ± 0.06 kT obtained with the nanopore method and here we pinpoint why tweezers overestimate the FE.

We are not the first to notice an overestimated FE when the FT is applied to optical tweezers pulling data. This is a common observation and the overestimated FE in the pulling experiments is usually attributed to the dissipation associated with stretching elastic handles, probes, and dragging beads through the fluid. The overestimation is typically corrected by subtraction, as explained in the methods section of Ref. [6] or in Refs. [7,48].

Unlike previous studies, we found that the overestimation observed in the optical tweezers experiment is not primarily attributable to factors such as beads, handles, tethers, or other experimental details. Instead, it stems from a conceptual issue related to how optical tweezers align with the assumptions that underlie the derivation of the FT in Eq. (2) [2,13].

In a comprehensive and detailed discussion, we will elucidate why the optical tweezers experiment fails to meet the assumptions inherent to the derivation of the FT. Specifically, tweezers sample only initially folded molecules and not molecules from the equilibrium ensemble, as mandated by the FT in Eq. (2). This deviation from equilibrium sampling results in the observed overestimation of ΔF. However, we will also address this issue and devise a solution to ensure equilibrium sampling in the tweezers experiment, ultimately achieving a high level of agreement between the nanopore and tweezers experiments.

Furthermore, in our analysis, we will delve into the impact of correcting measured work values by subtracting contri-

butions from elastic handles, probes, and beads on both the estimated mean work and the FE in the tweezers experiment. We will demonstrate that such corrections significantly influence the mean work but have minimal effects on the FE estimate with the FT when molecules are sampled from equilibrium. Notably, for far-from-equilibrium pulling, such as our experiments, the FE estimate proves to be more sensitive to the precise determination of the small fraction of unfolded molecules in equilibrium (ρ) than to corrections applied to the measured work values.

A. Reconstructing work distributions

The nanopore experiment detected molecules from equilibrium and we reconstructed bimodal work distributions [Fig. 3(a)] containing one peak for unfolded and one peak for folded fraction in equilibrium. The tweezers experiment detected only folded molecules and we reconstructed the single-peak work distribution [Fig. 4(e)]; however, such a work distribution is not compatible with the FT and it consequently led to the overestimated FE.

The fluctuation theorem in Eq. (2) requires work distributions from an equilibrium ensemble of molecules. For our hairpins, there are two distinct conformations in equilibrium: folded, where the DNA duplex is hybridized through H bonds, and unfolded, where H bonds are dissociated. The work distribution for molecules starting in equilibrium, $p(W)$, is a sum of conditional work distributions for molecules starting unfolded, $p_{s0}(W|\text{unfolded})$, and folded, $p_{s1}(W|\text{folded})$, weighted by their fractions in equilibrium, ρ and $1-\rho$, as

$$p(W) = \rho p_{s0}(W|\text{unfolded}) + (1-\rho)p_{s1}(W|\text{folded}). \quad (3)$$

The nanopore experiment detected folded and unfolded molecules and it provided $p(W)$ based on equilibrium as required for using the FT [Figs. 3(a) and 3(e)]. This led to the FE being practically independent of the pulling power in Figs. 3(b), 3(c), and 3(g). The tweezers experiment only detected folded molecules and provided $p_{s1}(W|\text{folded})$; hence, applying FT to the tweezers work PDF in Fig. 4(e) resulted in an overestimated FE.

1. Work distribution for molecules starting folded

For both experiments, the work distribution for molecules starting folded, $p_{s1}(W|\text{folded})$, was reconstructed by binning work values in a histogram and normalizing. For the number of traces we collected, work distributions from folded molecules in nanopore and tweezers experiments can be approximated as Gaussian. For a Gaussian distribution, we can express the exponential mean $\langle \exp(-\frac{W}{\text{kT}}) \rangle$ only in terms of the mean $\langle W \rangle$ and standard deviation σ^2 [5,13,33] as

$$\left\langle \exp\left(-\frac{W}{\text{kT}}\right)\right\rangle = \exp\left(\frac{\sigma^2}{2(\text{kT})^2} - \frac{\langle W\rangle}{\text{kT}}\right). \quad (4)$$

Both $\langle W \rangle$ and σ^2 are obtained by fitting the reconstructed distributions to the Gaussian function.

2. Work distribution for molecules starting unfolded

The work distribution for molecules starting unfolded, $p_{s0}(W|\text{unfolded})$, was more challenging to reconstruct in both experiments. In the tweezers experiment, no initially unfolded molecules [Fig. 4(h)] were detected. The tweezers experiment did not provide work values from initially unfolded molecules, nor could we find such values in other publications [3,5,6,8,10,11]. The nanopore experiment is more advantageous, because it was able to detect initially unfolded molecules in equilibrium [Fig. 2(c)]. Initially unfolded molecules activate the trigger and quickly translocate through the pore while we assign zero work and reconstruct the work distribution for the initially unfolded molecules as a peak at zero work, $p_{s0}(W|\text{unfolded}) \approx \delta(W)$, where $\delta(W)$ is the Dirac delta distribution. For the approximation with the Dirac delta distribution, the exponential mean reduces to

$$\left\langle \exp\left(-\frac{W}{\text{kT}}\right)\right\rangle \approx \langle \exp(0)\rangle = 1. \quad (5)$$

In the next section, we propagate the reconstructed work distribution to obtain the ΔF estimate.

B. Free-energy estimator

Equation (2) is a mathematical identity and it only holds for an infinite number of error-free work measurements, whereas experiments are not ideal and they collect a finite number of work measurements. In this section, we show how ΔF values are estimated from work measurements obtained in experiments.

Let us express the exponential averaging in Eq. (2) for a very large number ($N \to \infty$) of work measurements as a sum,

$$\frac{\Delta F}{\text{kT}} = -\ln \lim_{N\to\infty} \frac{1}{N}\sum_{i=1}^{N} \exp\left(-\frac{W_i}{\text{kT}}\right), \quad (6)$$

where W_i are individual work measurements indexed by i.

A naïve estimator involves substituting a finite number of work measurements directly in Eq. (6); however, it is recommended to avoid the naïve estimator, because it leads to a strong bias [33]. Instead, one should reconstruct a work distribution for molecules starting in equilibrium, $p(W)$, first, and then transform the work distribution to obtain ΔF [33]. Since we have already reconstructed work distributions $p(W)$, the next step is to propagate them to obtain ΔF.

Equation (2) generally requires work values from all molecules in equilibrium, regardless if they start folded or unfolded to give ΔF. We find it convenient to split the exponential mean in Eq. (2) to explicitly show work values from molecules starting unfolded, W_{s0}, and folded, W_{s1}, and weight them by ρ and $(1-\rho)$ as found in equilibrium:

$$\frac{\Delta F}{\text{kT}} = -\ln\left(\underbrace{\rho\left\langle \exp\left(-\frac{W_{s0}}{\text{kT}}\right)\right\rangle}_{\text{unfolded}} + \underbrace{(1-\rho)\left\langle \exp\left(-\frac{W_{s1}}{\text{kT}}\right)\right\rangle}_{\text{folded}}\right). \quad (7)$$

For molecules staring unfolded (W_{s0}), we approximated the work distribution with the Dirac delta in Eq. (5), while for molecules staring folded (W_{s1}), we approximated the work distribution as Gaussian in Eq. (4). Substituting Eqs. (5) and

(4) in Eq. (7), we obtain a robust FE estimator:

$$\frac{\Delta F}{\mathrm{kT}} \approx -\ln\left(\rho + (1-\rho)\exp\left(\frac{\sigma_{s1}^2}{2(kT)^2} - \frac{\langle W_{s1}\rangle}{kT}\right)\right). \quad (8)$$

The derived estimator in Eq. (8) uses three values: the mean work ($\langle W_{s1}\rangle$) and variance (σ_{s1}^2) for molecules starting folded are obtained from the fit to the Gaussian function, while ρ is obtained by counting the fraction of unfolded molecules in equilibrium. With the estimator in Eq. (8), the nanopore experiment provided FE values practically independent of the pulling power for both DNA hairpins [Figs. 3(b), 3(c), and 3(g)].

For our 10-bp hairpin sequence, the initially unfolded molecules are exponentially less likely (0.4%) to be detected than the initially folded molecules (99.6%). In practice the initially unfolded molecules remain hard to detect especially for more stable molecular structures, i.e., many biologically relevant DNA or RNA hairpins longer than 10 bp. The tweezers experiment also did not detect unfolded molecules and led to $\rho = 0$; hence, we further explore how the FE estimate is affected when it is based only on the initially folded molecules by setting $\rho = 0$ in Eq. (8) and expressing

$$\Delta F_{FB} \approx \langle W_{s1}\rangle - \sigma_{s1}^2/(2\ \mathrm{kT}). \quad (9)$$

The estimator based on folded molecules and $p_{s1}(W|\mathrm{folded})$ is labeled as ΔF_{FB} to distinguish it from the estimator based on equilibrium ΔF and $p(W)$.

1. Comparing free-energy estimators

The two FE estimators in Eqs. (8) and (9) are conceptually different, because the estimator in Eq. (8) is based on a work distribution from equilibrium, while the estimator in Eq. (9) is based on the work distributions from the folded ensemble. Applying the estimator in Eq. (8) to the nanopore data led to ΔF values practically independent of the pulling power as shown in Figs. 3(b) and 3(c) with data points around the horizontal line. Applying Eq. (9) to the nanopore data overestimated the FE and led to FE values strongly dependent on the pulling power in Figs. 3(h), because Eq. (9) does not use an equilibrium ensemble of molecules.

A similar problem occurred in the optical tweezers experiment. Tweezers detected only initially folded molecules and no unfolded molecules were detected ($\rho = 0$); hence, the estimator in Eq. (9) led to the work value above 17 kT. Nevertheless, Eq. (8) can be used to improve the tweezers estimate. We find that reconstructing the tweezers work distribution based on equilibrium [Fig. 4(f)] can be achieved by adding the second peak to represent the small fraction ($\rho = 0.4\%$) of unfolded molecules expected in equilibrium. After the reconstruction in Fig. 4(f) and using Eq. (8), the tweezers experiment leads to $\Delta F = 5.5 \pm 0.4$ kT and it agrees more closely with the value of 5.25 ± 0.06 obtained with the nanopore method without introducing any corrections to beads, tethers, or elastic handles.

We conclude that when the work distribution is based on equilibrium, two experiments agree within two significant digits; however, when the work distribution is obtained only from initially folded molecules, the two experiments disagree and the FE estimate strongly depends on the pulling power.

2. Crooks fluctuation theorem

The Crooks fluctuation theorem (CFT) presents an alternative method for estimating the FE change through work measurements in pulling experiments [6,14]. However, in this article, we do not delve into the CFT because neither the nanopore nor the tweezers experiment aligns with the two requirements for its application.

First, the CFT mandates the execution of both forward and time-reverse pulling protocols, while the Jarzynski FT in Eq. (2) only necessitates the forward protocol. Implementing the time-reverse voltage protocol in the nanopore experiment poses a significant technical challenge, and even when the voltage protocol is reversed [Fig. 2(b)], it does not return a molecule to its initial conformation. Consequently, the CFT is not directly applicable to the nanopore experiment.

While an optical tweezers experiment offers the possibility of implementing the time-reverse protocol, our tweezers experiment does not satisfy the second requirement of the CFT, which is to start and end with an equilibrium ensemble of molecules. Instead, our optical tweezers experiment initiates with the folded ensemble and concludes with the unfolded ensemble of DNA hairpins [Fig. 4(g)]. The Jarzynski FT, in contrast, only necessitates starting with an equilibrium ensemble [2].

To fulfill the requirement for Eq. (2), we reconstructed the tweezers work distribution in the forward protocol by supplementing it with the unfolded fraction ρ obtained through the nanopore experiment [Fig. 4(f)]. However, replicating a similar reconstruction in the time-reverse protocol is currently challenging. This is because it entails quantifying a small fraction $(1 - \rho_f)$ of pulling trials that conclude folded after pulling, whereas all our pulling trials resulted unfolded.

As work distributions in the time-reverse protocol are not accessible for our experiments, we are unable to apply the CFT to our measurements.

C. Domain

The derived FE estimator in Eq. (8) resulted in a very good agreement between experiments within two significant digits; however, Eq. (8) is not an exact mathematical identity like Eq. (2). The FE estimator in Eq. (8) is rather a very good approximation suitable for the set of conditions and parameters used in single-molecule pulling experiments. Next, we explore under what conditions the FE estimator in Eq. (8) improves and underperforms. We will show that the estimator underperforms for a slow, quasistatic, and near-equilibrium pulling, while it is very good for the fast or instantaneous pulling carried out very far from equilibrium.

1. Quasistatic pulling

Quasistatic or near-equilibrium pulling requires an extremely slowly process ($t_0 \to \infty$) at low power ($P \to 0$). In this regime, we would expect both initially folded and unfolded molecules to fluctuate between the folded and unfolded conformations many times as we slowly increase the laser distance λ [see the illustrations in Figs. 5(e) and 5(f)]. Eventually, when λ becomes sufficiently large, molecules become practically locked in their unfolded conformation.

In this limit, we expect it takes work to unfold an unfolded molecule, $\langle W_{s0}\rangle \neq 0$, although this statement may sound counterintuitive. Over sufficiently long pulling times, the initially unfolded molecule can spontaneously form H bonds and fold [Fig. 5(f)]; hence, the work is required for the dissociation and unfolding. Consequently, in the quasistatic pulling regime, approximating the work distribution for initially unfolded molecules with the Dirac delta is not appropriate and the estimator in Eq. (8) has a strong bias. In practice, it is challenging to run the tweezers experiment too slowly and observe many fluctuations between folded and unfolded conformation as λ increases, because of mechanical drifts and breaking of molecular tethers. The quasistatic regime is also less relevant for studying molecular processes, because molecular processes usually occur over fast times and very far from equilibrium.

2. Instantaneous pulling

We observe unfolding as a single abrupt step in the pulling trajectory, Fig. 4(b) at about 10 s, rather than multiple fluctuations between folded and unfolded conformations. This suggests that the pulling experiment occurs very far from equilibrium; hence, exploring very fast or instantaneous pulling is relevant for studying molecular processes. In the nanopore experiment, instantaneous or arbitrary far-from-equilibrium pulling can be achieved by further shortening the pulling time ($t_0 \to 0$) and increasing the maximal voltage above 200 mV, whereas in the tweezers experiment, moving the laser faster and increasing the maximal pulling distance λ increases power. In practice, driving arbitrarily far from equilibrium is more challenging because voltages above 200 mV can eject the nanopore and break the lipid bilayer, while the bead can escape the optical trap if the laser is moved too fast. Nevertheless, we can analytically explore this regime with Eq. (7).

When a folded molecule is instantaneously pulled with high power [Figs. 2(b) and 4(g)], the dissipation increases and very large work is required to dissociate H bonds and unfold. Work values W_{s1} for initially folded molecules in Eq. (7) become extremely large; hence, the negative exponent becomes zero in this limit, $W_{s1} \to \infty \Rightarrow \exp(-W_{s1}/\mathrm{kT}) = 0$.

Next, we consider an initially unfolded molecule [Figs. 2(c) and 4(h)], pulled in an instantaneous process with extreme power ($P \to \infty$). In such an instantaneous process there is no time for the molecule to spontaneously form H bonds. Unfolded molecules remain with dissociated H bonds [Fig. 4(h)]; hence, the work to dissociate is zero and the work distribution in this limiting case is exactly $p_{s0}(W|\text{unfolded}) = \delta(W)$. Since values W_{s0} for initially unfolded molecules are zero, the negative exponent in Eq. (7) becomes $W_{s0} = 0 \Rightarrow \exp(-W_{s0}/\mathrm{kT}) = 1$ in the instantaneous pulling process.

We combine work values for initially unfolded and folded molecules in Eq. (7) and obtain the FE estimate for the instantaneous pulling regime:

$$\frac{\Delta F}{\mathrm{kT}} = -\ln\left(\underbrace{\rho\cdot 1}_{\text{unfolded}} + \underbrace{(1-\rho)\cdot 0}_{\text{folded}}\right) \tag{10}$$

$$= -\ln\rho. \tag{11}$$

We find that for the instantaneous pulling, the HFE difference estimate solely depends on detecting the small fraction ρ of unfolded molecules in equilibrium, $\Delta F = -\mathrm{kT}\ln\rho$. Equation (11) is sometimes considered a definition of FE [3] and it can be used to calculate the FE by counting the unfolded fraction in equilibrium. Substituting our estimate $\rho = 0.4\%$ for the 10-bp DNA hairpin leads to $\Delta F = -\mathrm{kT}\ln(0.4\%) \approx 5.5$ kT and this value based on counting molecules in equilibrium close to the value of 5.25 ± 0.06 kT obtained from nonequilibrium work measurements.

The stability of a molecule can also be described with the FE parameter $\Delta G^o_T = -\mathrm{kT}\ln K$, where the equilibrium constant $K = [(1-\rho)/\rho]$ is defined as the ratio of folded and unfolded fractions in equilibrium. For $\rho = 0.4\%$, the FE parameter is $\Delta G^o_T \approx -5.5$ kT.

D. Improving free-energy estimators

In the previous section we showed that Eq. (8) gives the best FE estimate for an instantaneous pulling process, while it underperforms for slower and near-equilibrium pulling. Here, we discuss how to further improve the FE estimator in Eq. (8) in slower limits.

Improving the estimator in Eq. (8) requires a better reconstruction of the work distribution for molecules starting unfolded, $p_{s0}(W|\text{unfolded})$. In the presented derivation, we reconstructed it with the Dirac delta, $p_{s0}(W|\text{unfolded}) \approx \delta(W)$, and assigned zero work to all initially unfolded molecules. A better reconstruction of $p_{s0}(W|\text{unfolded})$ assumes that some of the initially unfolded molecules may temporarily refold during pulling in slower processes; hence, it assigns a small amount of work to some initially unfolded molecules. Obtaining a better $p_{s0}(W|\text{unfolded})$ in experiments is challenging due to limited statistics. Nevertheless, we can propose the exponential distribution $p_{s0}(W|\text{unfolded}) \approx \langle W_{s0}\rangle^{-1}\exp(-W/\langle W_{s0}\rangle)$ for this reconstruction, where the average work for molecules starting unfolded is not zero ($\langle W_{s0}\rangle \neq 0$) and also can depend on the loading rate. The exponential distribution has a positive tail to account for nonzero work in case there is temporary refolding; nevertheless, better reconstruction of $p_{s0}(W|\text{unfolded})$ cannot be provided with experiments presented here due to technical limitations and that our reconstruction with the Dirac delta already leads to a reasonable agreement between the two experiments.

VI. CORRECTIONS TO WORK VALUES

Nanopore and tweezers experiments pull different molecular constructs. The nanopore experiment pulled only DNA hairpins, while the tweezers experiment pulled DNA hairpins together with attached elastic handles and beads. On average, work values obtained in the tweezers experiment ($\approx$17.2 kT) are higher than the work values obtained with the nanopore ($<$11.1 kT), because the tweezers experiment requires work to stretch elastic handles in addition to work to dissociate H bonds. Nevertheless, both experiments lead to an agreement in ΔF values of 5.5 and 5.25 kT, respectively, when using the estimator in Eq. (9) without introducing corrections.

In this section, we further explore how corrections to measured work values affect the mean work $\langle W\rangle$ and the

TABLE I. Corrections applied to the work values in the tweezers experiment strongly affect the mean work, while corrections below 8 kT practically do not affect ΔF. Percent correction was calculated as $-\ln \rho/W_{CR}$. Corrected work $\langle W\rangle$/kT was calculated with Eq. (13), and corrected ΔF/kT was calculated with Eq. (14) with values $\langle W_{s1}\rangle = 17.248$ kT, $\sigma_{s1}^2 = 1.16205$ kT^2, and $\rho = 0.4\%$.

W_{CR}/kT	Percent	$\langle W\rangle_{\rm cor}$/kT	$\Delta F_{\rm cor}$/kT
0	0%	17.17	5.52144
0.5	9%	16.68	5.52143
1	18%	16.18	5.52142
2	36%	15.18	5.5213
4	72%	13.19	5.5206
8	145%	9.21	5.4794
12	217%	5.22	4.3152
16	290%	1.24	0.6631
-8	145%	25.15	5.52146

FE estimate ΔF. We show that corrections to work values strongly affect the mean work $\langle W\rangle$, but they have little effect on the ΔF estimate with the FT.

A. Corrections in the tweezers experiment

The example molecular trajectory in Fig. 4(b) resulted in a work value of approximately 18 kT. In our analysis, no corrections were made to account for elastic contributions, and work values were directly used to estimate both the mean work $\langle W\rangle$ and the FE ΔF through Eq. (9). In our subsequent analysis, we introduce arbitrary work corrections denoted as W_{CR} to the measured work values W_{s1}. We then calculate both $\langle W\rangle$ and ΔF after applying these corrections. This approach allows us to quantify the impact of corrections on both $\langle W\rangle$ and ΔF in the far-from-equilibrium regime where our experiments operate.

Let us first evaluate how an applied correction W_{CR} to the measured work value W_{s1} affects the mean work $\langle W\rangle$ in the tweezers experiment. The mean work before any correction is calculated as

$$\langle W\rangle = \underbrace{\rho\langle W_{s0}\rangle}_{\text{unfolded}} + \underbrace{(1-\rho)\langle W_{s1}\rangle}_{\text{folded}}, \tag{12}$$

where $\langle W_{s0}\rangle$ and $\langle W_{s1}\rangle$ are mean work for molecules starting unfolded and folded, while ρ is the unfolded fraction in equilibrium. The mean work for molecules starting unfolded is very small ($\langle W_{s0}\rangle \approx 0$) in a far-from-equilibrium process.

Let us now apply a constant correction W_{CR} to measured work values W_{s1} in Eq. (12) by subtracting $\langle W_{s1} - W_{CR}\rangle = \langle W_{s1}\rangle - W_{CR}$, substituting $\langle W_{s0}\rangle \approx 0$, and evaluating the mean work after the correction, $\langle W\rangle_{\rm cor}$, as

$$\langle W\rangle_{\rm cor} \approx (1-\rho)(\langle W_{s1}\rangle - W_{CR}). \tag{13}$$

For the 10-bp hairpin, correcting measured work values W_{s1} by W_{CR} affects the mean work by $0.96\% W_{CR}$. Table I shows calculated mean work after corrections, $\langle W\rangle_{\rm cor}$, for several W_{CR} values in the range from 0 to 16 kT applied to the optical tweezers data set. From Table I, we conclude that applying corrections to measured work values strongly affects the mean work.

Next, let us evaluate how an applied correction W_{CR} to the measured work value W_{s1} affects the FE estimate ΔF. In the FE estimator in Eq. (9), we subtract the correction W_{CR} from the measured work value W_{s1} and obtain the estimator with the correction term,

$$\frac{\Delta F_{\rm cor}}{\rm kT} \approx -\ln\left(\rho + (1-\rho)\exp\left(\frac{\sigma_{s1}^2}{2(kT)^2} - \frac{\langle W_{s1}\rangle - W_{CR}}{\rm kT}\right)\right). \tag{14}$$

The FE estimator in Eq. (14) based on the FT is less sensitive to the applied correction W_{CR}. Table I shows calculated $\Delta F_{\rm cor}$ values for several corrections in the range from 0 to 16 kT. With or without corrections of up to 8 kT applied to the measured work values, we obtain virtually the same FE value. For instance, without corrections, ΔF is approximately 5.52 kT, and after applying an 8-kT correction to measured work values, $\Delta F_{\rm cor}$ is around 5.48 kT. Since the correction of 8 kT affected FE by less than 0.05 kT, we conclude that such corrections are not necessary. Instead, the key focus should be on accurately determining the fraction of unfolded molecules in equilibrium, ρ.

We conclude that corrections applied to measured work values strongly affect the mean work $\langle W\rangle$, while such corrections have small effect on the FE estimate with the FT as long as molecules are sampled from equilibrium. Because the effect of corrections is small when ΔF is calculated with FT, we applied no corrections to work values in our analysis.

B. Pore protein and DNA interactions

While the nanopore measurement does not involve beads or elastic handles, other experimental factors may influence the measured work values and the estimated FE. When a folded DNA hairpin enters the nanopore [Fig. 2(b)], the interaction between the pore protein and DNA could potentially destabilize H bonds, resulting in a lower work required to dissociate these bonds. Therefore, it is crucial to investigate how corrections to the protein-DNA interaction may affect $\langle W\rangle$ and ΔF.

In the optical tweezers experiment, the presence of elastic handles introduces additional work, denoted as W_{CR}, which we corrected by subtracting it from the work values. Conversely, in the nanopore experiment, the interaction between the pore protein and DNA might lead to a reduction in work. Therefore, we explored the possibility of correcting this effect by adding W_{CR} to the work values. We conducted a similar analysis of corrections as in the tweezers experiment, with the key difference being that we used a correction term (W_{CR}) of the opposite sign in Eqs. (13) and (14). For instance, without corrections, ΔF is approximately 5.52 kT, and after applying a -8 kT correction to measured work values, $\Delta F_{\rm cor}$ remains around 5.52 kT, while the mean work increases to 25.15 kT.

Introducing corrections in the nanopore experiment yielded outcomes akin to those observed in the tweezers experiments. Corrections significantly affected the mean work but had minimal impact on ΔF due to the negative exponential averaging in Eq. (14). Since the nanopore FE estimator also displayed insensitivity to corrections, we refrained from applying any corrections in our analysis of nanopore data.

VII. COMPARISON WITH LITERATURE

We find it important to emphasize the progress made and explain key differences between ours and other famous experiments utilizing FTs [5,7].

With both nanopore and tweezers experiments, we presented two major improvements relative to the experiment by Liphardt *et al.* [5]—one of the first tests of the FT with biomolecules. First, we used the stochastic work definition and showed how to integrate the pulling power over time to obtain the work value with Eq. (1), whereas Ref. [5] calculates work with a force integral. The force integral is not compatible with the FT in Eq. (2) and not expected to lead to the correct FE value [17,23,24]. Second, Liphardt *et al.* [5] sampled only initially folded molecules and estimated the FE from a single-peak Gaussian distribution without specifying the unfolded fraction in equilibrium. We sampled molecules from equilibrium, determined the unfolded fraction ρ, and reconstructed a bimodal work distribution to represent the equilibrium ensemble required for using the FT.

Another notable study by Harris *et al.* [7] used AFM to pull only folded proteins and this consequently led to the overestimated FE as explained in Ref. [48]. We also find the FE is overestimated when only folded molecules are pulled and FT applied to $p_{s1}(W|\text{folded})$; however, we showed that including a small fraction of initially unfolded molecules in the work distribution leads to the FE practically independent of the pulling power or the experimental setup used.

A. Comparison with computational tools

Computational tools are very helpful in predicting the structure and stability of folded DNA and RNA molecules [49,50]. The Mfold tool [49] can calculate the ΔG quantity online after a user specifies the sequence, sodium [Na^+] and magnesium [Mg^{++}] concentrations, and temperature. For our 10-bp DNA hairpin, 500 mM [Na^+], and 22 °C, Mfold calculated 22 kT, a value higher than 5.5 kT we measured in 500 mM [K^+], pH 9.0, and 22 °C. The computed value of 22 kT implies an extremely small unfolded fraction of $e^{-22} \approx (2.8 \times 10^{-8})\%$, while we detected 0.4% of unfolded molecules in equilibrium. The possible reason for the difference between the measured and computed estimates is a consequence of the two using and assuming different conditions. First, we measured in potassium buffer, while Mfold assumes a sodium buffer. Second, we used an alkaline buffer of pH 9.0, while the Mfold tool does not explicitly account for pH and the concentration of hydroxide ions, [OH^-]. The concentration of hydroxide ions, [OH^-], affects the fraction of unfolded molecules in equilibrium. The abundance of hydroxide ions [OH^-] at high pH destabilizes H bonds, makes the DNA duplex susceptible to alkaline denaturation, and shifts the equilibrium towards more unfolded molecules [51–53]. Third, Mfold estimates are more accurate around 50 °C and they become less accurate as the temperature deviates from 50 °C [50], while our measurements are at 22 °C.

B. Interpretation

We showed how to measure ΔF with nanopores and demonstrated a consistency between the nanopore and tweezers experiments, but our findings can also provide additional interpretations of important theoretical results in nonequilibrium statistical mechanics. We obtained the ΔF value via the FT by reconstructing work distributions $p(W)$ and also calculated $\Delta F = -\text{kT} \ln \rho$ from the fraction of unfolded molecules in equilibrium. Both approaches practically led to the same ΔF value, but they both required us to detect unfolded and folded molecules and provide information about the fraction of unfolded molecules in equilibrium, ρ. Inspired by the title of Ref. [5]: "Equilibrium Information from Nonequilibrium Measurements in an Experimental Test of Jarzynski's Equality," we explain how equilibrium information about our DNA hairpin is obtained. We found the equilibrium information about the fraction ρ is collected by the instrument through detecting folded and unfolded molecules in equilibrium. A nonequilibrium measurement and work distribution $p_{s1}(W|\text{folded})$ based on pulling solely folded molecules was not able to provide the correct ΔF, ρ, or any other equilibrium information in a fast process.

We find the interpretation of theoretical results very useful, because with the adequate interpretation we can formulate better questions to address with experiments. Next, we will show that work measurements obtained with nanopores are better utilized for comparing FEs of two different hairpin sequences at fast times, rather than finding the FE for each sequence. We also propose several future applications of the nanopore method.

VIII. APPLICATIONS OF THE NANOPORE METHOD

The nanopore method, with its unique features, can sample from equilibrium, estimate, and detect the unfolded fraction ρ for less stable hairpins under 10 bp; however, determining ρ for more stable molecules is not always feasible with a few thousand pulls. Even when ρ is determined, the exponential averaging in Eq. (2) puts most of the weight on the fraction ρ under the near-zero peak, while precise work measurements for folded molecules remain unutilized for estimating ΔF via FT. This makes tweezers and nanopore methods impractical in the high-power limit, where they are typically operated. When ρ is not accessible and initially unfolded molecules not detected, the nanopore method can still utilize work measurements and distributions from initially folded molecules and provide very useful relative FE measurements between two molecules at finite times. For initially folded 10- and 7-bp hairpins, we reconstructed the work cumulative distribution function (CDF) using the sorting method [Fig. 4(i)] [54]. The shift in CDFs quantifies the difference in the stability and shows that the 7-bp hairpin is less stable by $\Delta F_{10} - \Delta F_7 \approx 2$ kT [Fig. 4(i)]. Relative comparison needed moderate statistics of only ≈200 work measurements, unlike counting ρ which required over 1000 measurements. Many other measurements of interest in biophysics can be reduced to the problem in Fig. 4(i), such as comparing RNA complexes with or without ligands, effects of different mutations in DNA/RNA sequences, comparing the binding energy between proteins and nucleic acids, and even comparing how point mutations in proteins affect their binding affinity. For example, it was recently reported that the H93A mutation in *Geobacillus stearothermophilus* PcrA helicase motor protein

lowers its binding energy to ssDNA [55] and the nanopore method allows one to pull an ssDNA bound to the helicase to directly quantify how the mutation changed the binding energy. Other advantages of the nanopore method include the ability to sample a fresh molecule for each pull, while tweezers and AFM repetitively pull the same molecule many times. Sampling a fresh molecule is more convenient in a situation when each pull irreversibly damages the molecule or molecular construct. For molecules that slowly equilibrate, tweezers and AFM require long waits between pulls, while the nanopore method samples a fresh molecule from equilibrium with no need to wait between pulls.

IX. SUMMARY

In this article, we used nanopores to quantify the stability of folded biomolecules and we resolved the issue of equilibrium sampling in single-molecule pulling experiments. We pulled DNA hairpin molecules through a protein nanopore, measured work in kT units, and applied the Jarzynski fluctuation theorem to find the change in the free energy. We also pulled molecules with optical tweezers and obtained the free energy. The free-energy change obtained in the nanopore experiment is practically independent of the pulling power and it further agrees with the optical tweezers measurement as long as molecules are sampled from equilibrium. We found that introducing corrections to measured work values strongly affects the mean work in pulling experiments, but has practically no effect on the free-energy estimate with the fluctuation theorem. The free-energy estimate is rather sensitive to determining the small fraction of unfolded molecules in equilibrium and less sensitive to the presence of elastic handles in the tweezers experiment or interactions between the pore protein and nucleic acids in the nanopore experiment. Even if rare unfolded molecules are not detected in equilibrium, the nanopore method can still be applied to determine relative FEs in many biophysical systems. In future studies, the nanopore method can be applied to probe interactions in protein and DNA complexes and be used to study optimization and various pulling protocols.

ACKNOWLEDGMENTS

We thank Karel Proesmans for reading the manuscript and Chris Jarzynski, Nancy Forde, Massimiliano Esposito, John Bechhoefer, David Sivak, Artemy Kolchinsky, and Margaret Johnson for helpful discussions. We also thank Jens Gundlach's laboratory at the University of Washington for the experiment design and Sangwoo Park for suggesting tweezers control. We acknowledge the Howard Hughes Medical Institute for support and funding from the National Institutes of Health (R35 GM 122569) to T.H., NSERC Canada Postdoctoral Fellowship to M.G., and BDP Summer Undergraduate Research stipend to J.Z.

APPENDIX

1. Apparatus

Our apparatus consists of the Teflon sample holder and a power supply connected to the electrodes. We refer to the

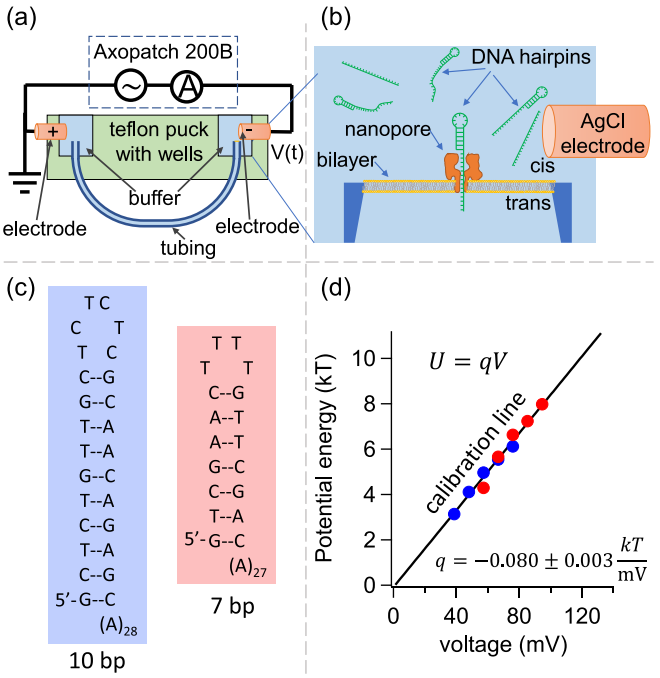

FIG. 6. Experimental setup and calibration. (a) The nanopore setup consists of two chambers connected with tubing and filled with KCl buffer. Each chamber has one AgCl-pellet electrode connected to an amplifier. The tubing in the *cis* chamber shrinks to about 20 μm to support a lipid bilayer. (b) The lipid bilayer contains one α-hemolysin nanopore. DNA hairpins at ≈1 μM concentration are added to the *cis* chamber above the bilayer. (c) Two DNA hairpin sequences in folded configurations. (d) Nanopore calibration line links the applied voltage in mV to the potential energy in kT via the effective charge q. Design of figures in parts (a) and (b) is inspired by Ref. [27].

Teflon sample holder as a "puck." The puck is colored in green in Fig. 6(a) and it consists of two wells (light blue) connected by a tubing. Each well contains between 60 and 70 μl of the buffer solution. The puck is custom made by the Physical Sciences Machine Shop at Johns Hopkins University. Two wells are connected with Zeus PTFE/FEP Dual Shrink Tubing [part no. SMDT-130; Fig. 6(a)]. The tubing shrinks to ≈20 μm in the *cis* well to create an aperture for supporting the bilayer [Fig. 6(b)]. Molecules are loaded in the *cis* well, above the lipid bilayer. We use AgCl-pellet electrodes from A-M systems (part no. 550010). The electrodes are coated by PTFE/FEP Dual Shrink Tubing (part no. SMDT-036) that also seals the electrode opening on the puck. The power supply, model Axopatch 200B, controls the voltage and measures the electric current or conductance of the nanopore with two AgCl electrodes, one on each side of the membrane. The Axopatch 200B is connected to a PC via a DAQ card. A control software also implements a feedback and is written in LABVIEW. Our experimental setup and lipid bilayer preparation protocols are similar to the setup in Ref. [27].

DNA hairpin-forming sequences are illustrated in Fig. 6(c). We purchased DNA oligos from IDT (Integrated DNA Technologies.) DNA oligos are diluted in 500 mM KCl + 50 mM HEPES pH 9.0 buffer, then heated to 95 °C and quenched to 4 °C. We perform the experiment at 22 °C in 500 mM KCl +

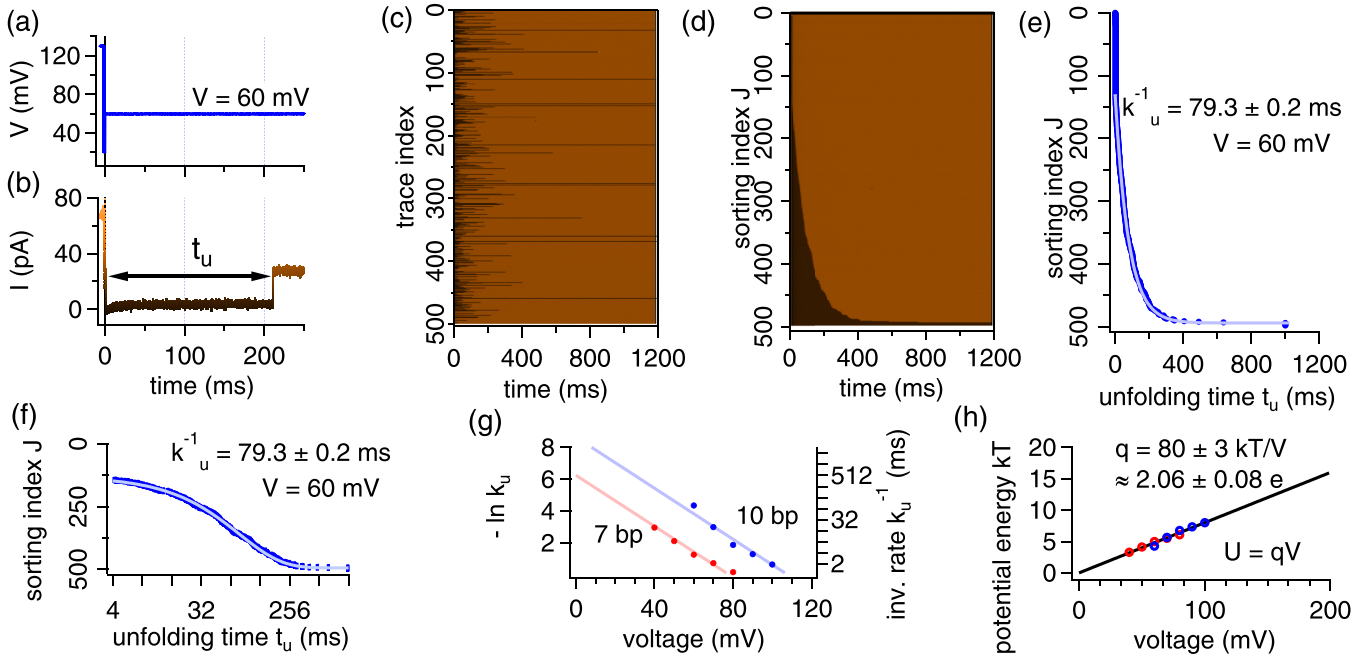

FIG. 7. Constant-voltage ($\frac{dV}{dt} = 0$) calibration. (a) Constant voltage measurement consists of searching for molecules $t < 0$ and pulling $t \geqslant 0$. (b) Drop in current before $t < 0$ ms triggers lowering the voltage to 20 mV and setting the voltage to 60 mV at $t = 0$. Sudden increase in the electric current at ≈200 ms indicates a molecule's unfolding and translocating through the pore. (c) Each horizontal line represents a trace indexed from 1 to 500. (d) Sorted current traces according to the unfolding times. (e) Extracted unfolding times from the part in (d) are fit to the exponential distribution. Unfolding rate k_u^{-1} at the fixed voltage is obtained. (f) linear-log plot of graph in (e). (g) Repeating parts (b)–(f) for five different voltages and two hairpin sequences. The effective charge is obtained from the linear fit. (h) The calibration line tells how much the applied voltage in mV increases the potential energy of molecule in kT units.

50 mM HEPES pH 9.0 buffer [18]. Both oligos, 7- and 10-bp-long hairpins, have the same effective charge q [Fig. 6(d)], because they both have the same single-stranded overhang in the nanopore.

2. Nanopore calibration

The calibration procedure measures a molecule's effective charge under the same experimental condition used to obtain the FE difference (500 mM KCl buffer at 22 °C). Measuring the effective charge of $q = -0.080 \pm 0.003$ kT/mV $= 2.06 \pm 0.08e$ is based on 5000 pulls. Figure 7 shows each step of the calibration procedure in the constant-voltage mode. We apply >120 mV to the open pore to capture a DNA molecule. A molecule in the pore is detected as a drop in the current by a National Instruments data acquisitions (DAQ) card at 0.2 MHz frequency. The amplifier triggered by a DAQ card lowers the voltage to 20 mV within 5 μs after a molecule is detected. We keep the voltage at 20 mV for 1 ms, before we set the desired constant voltage.

Figure 7(a) shows the applied constant voltage of 60 mV and Fig. 7(b) shows the measured current signal through the nanopore. Between 0 and $t_u \approx 200$ ms, the electric current is low, indicating that the molecule is blocking the pore. The molecule unfolds at $t_u \approx 200$ ms in Fig. 7(b), detected as a switch to the high current. This switch can also occur due to the diffusion escape of a DNA hairpin back to the negative electrode compartment, but such escape is extremely unlikely here because it occurs on a 100-s timescale [18,28,29]. We can keep a folded DNA hairpin molecule in the pore, because a 28-nucleotide-long single-stranded overhang enters deep inside the pore. We repeated the measurement in Fig. 7(b) 500 times and collected 500 traces.

In Fig. 7(b), the plot becomes less practical for displaying 500 pulling traces. To address this limitation, we introduce a color-coded plot in Fig. 7(c). In this representation, each horizontal line corresponds to one pulling trace, indexed from 1 to 500. The color of each horizontal line corresponds to the value of the electric current, and it changes from dark (black) to light (brown) to signify the switch in electric current after unfolding. Figure 7(c) provides a convenient visual representation that allows for the inspection and analysis of a large number of single-molecule traces.

Subsequently, in Fig. 7(d), we sorted these traces based on the unfolding time (t_u) and assigned each trace a new index (J) after sorting, labeled as "sorting index J" on the y axis [54]. Figure 7(d) also illustrates that the transition from a blocked (dark) to an open pore (light) follows an exponential distribution.

We further extracted the unfolding times t_u from Fig. 7(d) and displayed them in Fig. 7(e) with solid markers. To obtain the unfolding rate from the plot in Fig. 7(e), we fit data with exponential function $J = J_0 + A\exp(-t_u/\tau_0)$, where J_0, A, and τ_0 are fit parameters and the fit is plotted with the solid line in Fig. 7(e) [54]. From the fit, we obtained the inverse unfolding rate of $k_u^{-1} = \tau_0 = 79.3 \pm 0.3$ ms for the constant voltage of 60 mV. Figure 7(f) shows the fit from Fig. 7(e) on the linear-log plot indicating that the exponential model is appropriate for our data set.

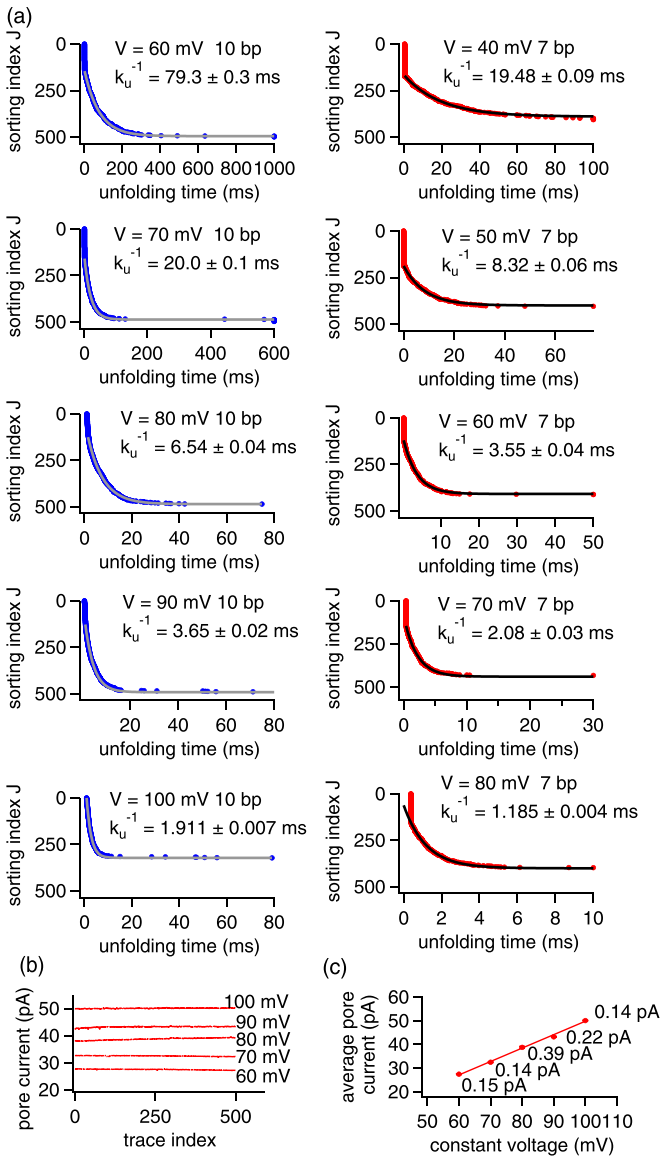

FIG. 8. Unfolding rates and the open pore stability. (a) Unfolding rates at different constant voltages for both DNA hairpins were used to estimate the molecule's effective charge. (b) Open pore current after a molecule translocates through the pore for approximately 500 pulls at each constant voltage. (c) Open pore current versus the applied voltage shows linear dependence. Values next to markers show standard deviation in current measurements at each voltage.

We repeat the entire procedure [Figs. 7(b) to 7(f)] for five constant voltages (60, 70, 80, 90, and 100 mV) for a 10-bp sequence (blue) and five constant voltages (40, 50, 60, 70, and 80 mV) for a 7-bp sequence (red) and show fit results in Fig. 8(a). Each fit provided the unfolding rate and we show rates $-\ln k_u$ and k_u^{-1} in Fig. 7(g) versus the applied constant voltage.

From the linear fit $-\ln k_u = Y - qV/\mathrm{kT}$ in Fig. 7(g), we find the effective charge q and the intercept on the y axis, Y. The effective charge q is a property of single-stranded DNA in the pore and the pore's size, and is independent of the hairpin stem length; hence, we measure the same q for both sequences despite the different rates. We obtain $q = -0.080 \pm 0.003\ \mathrm{kT/mV} = 2.06 \pm 0.08e$, where e is the unit charge, using an α-hemolysin (αHL) pore in our buffer condition. We employ q as a calibration coefficient determining how much the applied voltage in mV increases the potential energy in kT units. Figure 7(h) shows the calibration line, $U/\mathrm{kT} = qV/\mathrm{kT} = Y + \ln k_u$. The maximal potential energy is limited to 16 kT, because voltages higher than 200 mV can disrupt the lipid bilayer and eject the pore.

3. Total power

In the nanopore experiment, the electric current signal serves the purpose of determining whether the pore is blocked by a molecule and is also employed to measure unfolding times. However, it is important to note that the electric current value, typically measured in picoamperes, is not directly used to calculate power or the work needed to unfold a single molecule. Instead, pulling power and work are estimated based on the molecule's effective charge (q) and the applied voltage (V).

The total dissipation in the nanopore experiment over a time period (t_x) can be calculated as $W_{\mathrm{elec}} = IVt_x$, where I represents the current flowing through the nanopore, and V denotes the applied voltage. For instance, during a 100-ms-long experiment where the average current through the nanopore is $I = 50$ pA and the applied voltage is $V = 100$ mV, the total electric work amounts to $W_{\mathrm{elec}} = 5 \times 10^{-13}$ J, which is approximately 1.22×10^8 kT.

It is noteworthy that the total dissipation in the nanopore system is substantially greater, by eight orders of magnitude, than the dissipation associated with unfolding a single molecule. This is because the macroscopic current I encompasses the transport of all charged ions in the buffer solution. Nonetheless, through precise quantification of the molecule's effective charge and the use of Eq. (1), we are able to effectively isolate the work required to unfold a single molecule from the total work needed to sustain the nanopore measurement.

4. Measurement stability

The stability of both the nanopore and optical tweezers setups plays an important role in ensuring consistent measurements and the reproducibility of results. For the nanopore experiment, we determine the stability by estimating deviations and drifts in the open pore current during our experiments. For the optical tweezers experiment, we determine the stability by measuring deviations and drifts in the position of the laser focus. We will show that the nanopore experiment remains stable with drifts in the electric current between 0.26% and 1%, depending on the pulling rate, while drifts in the position of the laser focus are in the range from 0.48% to 0.56%.

a. Stability of the nanopore measurement

We assess the stability of the nanopore setup in a multistage evaluation process. Upon forming a lipid bilayer, we assess whether it effectively seals the opening between two chambers by measuring a giga-ohm (GΩ) resistance. By applying a voltage of ±200 mV across the bilayer and monitoring the current

typically below ±1 pA we determine the bilayer resistance. A high-quality bilayer exhibits GΩ resistance and can withstand more than 1500 pulls. After 2000 pulls, the bilayer should be replaced, because some degradation may become evident, leading to increased current "leaks" noise through the bilayer.

In our buffer solution, applying a voltage of 100 mV across the αHL pore results in an approximate current of 50 pA. Figure 8(c) illustrates the linear dependence between the open pore current and the applied voltage across the nanopore. To assess the long-term stability of the nanopore measurements, we monitor the open pore current after each pull. Following a molecule's translocation through the pore [as shown in Fig. 7(d)], the open pore current stabilizes at approximately 27.5 pA for applied 60 mV. Figure 8(b) presents the open pore current data for 500 pulls at five constant voltages. At each voltage, we determine the mean and the standard deviation [Fig. 8(c)]. Figure 8(c) further demonstrates both a linear dependence on applied voltage and a small standard deviation between 0.11 and 0.39 pA. In terms of percentage, the open pore current deviates between 0.26% and 1%, as obtained by dividing the standard deviation by the average current. These observations indicate the remarkable stability of our electric measurements in the biophysical setting.

b. Stability of the tweezers measurement

The stability of the commercial optical tweezers setup C-trap by Lumicks is also tested in several stages. After trapping two beads, C-trap performs the automatic calibration by analyzing the power spectrum of the bead-position measurement. The calibration algorithm uses the corner frequency to estimate the trap stiffness at the fixed laser-focus position. The increase in low frequencies in the power spectrum indicated drifts, but estimating drifts in micrometers from the power spectrum is challenging. We rather directly measure how the laser position drifts from nominal values. We repetitively move the laser focus from a nominal starting position at 6.0 μm to an ending position at 6.5 μm to pull the molecule [Fig. 4(c)]. However, from measurements, we obtained the mean starting position of 6.0336 ± 0.0004 μm and the mean ending position is 6.5315 ± 0.0005 μm. Drifts during the tweezers measurement are estimated as a difference between the nominal and average measured position, and for our position measurement we obtained 0.0336 and 0.5315 μm. We can also find the percent drift by dividing the drift by the laser position. Percent drifts are 0.48% to 0.56%.

In both experiments, we observed comparable drifts below 1%.

5. Stochastic versus mechanical work definition

In the optical tweezers literature, two different work definitions can be found. To obtain the work value from the trajectory in Fig. 4, we can either integrate the pulling power in time, $\int P dt$, or we can integrate the force over the moving laser position, $\int f d\lambda$. When applied to the same tweezers trajectory in Fig. 4, the power integral leads to a work value of about 18 kT, while the force integral leads to a work value above 59 kT. In this section we show how to evaluate work with both definitions, we provide more details about the integration scheme, and we discuss differences.

The stochastic work definition in Eq. (1) integrates power in time and such work definition is used in our nanopore, our tweezers, the tweezers experiment in Ref. [8], and experiments in Refs. [31,37–40]. Theoretical studies also recommend using the work definition in Eq. (1) in the context of FTs for estimating ΔF [2,13,17,23].

A more popular work definition in the biophysics literature [5–7,9,10] uses the force integral, i.e., Eq. (2) in Ref. [5], Eq. (2) in Ref. [9], Eq. (S4.1) in Ref. [11], Eq. (2) in Ref. [6], Eq. (5) in Ref. [10], etc. We refer to it as the mechanical work definition, because a similar expression is called work in many textbooks on mechanics [17]. This definition,

$$W_{0_i} = \int_{\lambda_0}^{\lambda_1} \left.\frac{\partial U(x,t)}{\partial x}\right|_{t_i} d\lambda = \int_{\lambda_0}^{\lambda_1} f_i d\lambda, \tag{A1}$$

integrates force f_i over the laser position λ, where λ_0 and λ_1 are initial and final laser positions, and i is the index of a pull. The mechanical work definition in Eq. (A1) does not appear in the discussions about microscopic foundations of macroscopic thermodynamics, it was not assumed in the derivation of the FT, and it is not expected to lead to the true ΔF value via the FT [17,23,24].

We apply both work definitions to our example trajectory in Fig. 4 and compare the obtained values. In the tweezers experiment, the pulling protocol in Fig. 4(a) moves the laser position λ from $\lambda_0 = 6.0$ μm to $\lambda_1 = 6.5$ μm over 12 s at a constant speed of 0.041 μm/s. We record the bead trajectory in Fig. 4(b) and observe unfolding at $t_u = 10$ s as a discontinuity in the position.

We obtain the stochastic work with the power integral in Eq. (1) in three steps.

(1) Estimate the potential energy: The optical trap imposes a harmonic potential $U(\Delta X) = \frac{1}{2}\kappa(\Delta X)^2$ and in our case the stiffness is $\kappa = 0.31$ pN/nm and 1 kT = 4.114 pN nm. For the trace in Fig. 4(b) the calculated potential energy versus time is shown in Fig. 4(d).

(2) Estimate the pulling power: We calculate the power, $P = \frac{\partial U(x,t)}{\partial t}|_x$, as the slope of the plot in Fig. 4(d), and show it in Fig. 5(a). Nanopore applies a constant pulling power, while the tweezers pulling power is a nonlinear function [Fig. 5(a)]. The power starts near zero while handles are relaxed and then it increases as handles are stretched.

(3) Calculate the stochastic work value: The power is integrated during the unfolding time, $P = \int_0^{t_u} P(t)dt$. The integrated area under the power is marked in Fig. 5(b) and it leads to the value of ≈18 kT for this example trajectory. No corrections are introduced. The unfolding time (t_u) is stochastic and it further leads to a distribution in work values. An important case is for the initially unfolded molecule, when $t_u = 0$ and the integral leads to zero work, $P = \int_0^0 P(t)dt = 0$, without the need to introduce any corrections. This is also a natural result for fast pulling, because we do not expect to spend work to unfold an already unfolded molecule; however, in the slow limit, an initially unfolded molecule may spontaneously refold during pulling while still requiring some work. To avoid spontaneous refolding, it is better to pull molecules faster and with more power.

Next, we obtain the mechanical work with Eq. (A1) for the same trajectory in Fig. 4. We do not find the work definition in

Eq. (A1) meaningful in the context of single-molecule pulling experiments. The work definition in Eq. (A1) is popular in the biophysics literature; hence, we evaluate it for our trajectory and further compare with the work definition in Eq. (1).

(1) Calculate force: For the position measurement in Fig. 4(b), we calculate the force $f = \kappa \Delta X$ and show it versus the laser position in Fig. 5(c). The obtained plot shows two "branches." The top branch corresponds to molecules in the folded conformation, while the bottom branch corresponds to molecules in the unfolded conformation. Unfolding is detected in a sudden switch from the folded to the unfolded branch at $\lambda_u \approx 6.44$ μm.

(2) Integrate force: The total work integral is obtained as the area under the folded branch from $\lambda_0 \approx 6$ μm to $\lambda_u \approx 6.44$ μm, shaded in Fig. 5(c). The integrated area leads to the total work value of $W_{\text{tot}} = 358.1$ kT. The value via the force integral is much higher than the value obtained with the stochastic work definition in Eq. (1).

(3) Work correction: The work correction is obtained by integrating the area under the bottom or unfolded branch, shaded in Fig. 5(d). This area is frequently associated with the work to stretch the elastic tethers and it leads to the value of $W_c = 298.7$ kT for our trace. To obtain the work to unfold the molecule, we subtract the correction from the total work and obtain the value $W_0 = W_{\text{tot}} - W_c = 358.1\,\text{kT} - 298.7\,\text{kT} = 59.4$ kT.

The work value via Eq. (A1) is higher than the work value obtained with Eq. (1). For both our experiments, the reported work values and free energies were obtained with Eq. (1) and not Eq. (A1).

[1] P. Atkins and J. D. Paula, *Physical Chemistry*, 7th ed. (W. H. Freeman, New York, 2002).
[2] U. Seifert, Rep. Prog. Phys. **75**, 126001 (2012).
[3] M. Woodside and S. Block, Annu. Rev. Biophys. **43**, 19 (2014).
[4] P. Selvin and T. Ha, *Single-Molecule Techniques: A Laboratory Manual* (Cold Spring Harbor Laboratory Press, Cold Spring Harbor, NY, 2008).
[5] J. Liphardt, S. Dumont, S. Smith, I. Tinoco, Jr., and C. Bustamante, Science **296**, 1832 (2002).
[6] D. Collin, F. Ritort, C. Jarzynski, S. B. Smith, I. Tinoco, Jr., and C. Bustamante, Nature (London) **437**, 231 (2005).
[7] N. C. Harris, Y. Song, and C.-H. Kiang, Phys. Rev. Lett. **99**, 068101 (2007).
[8] A. Gupta, A. Vincent, K. Neupane, H. Yu, F. Wang, and M. Woodside, Nat. Phys. **7**, 631 (2011).
[9] P. Heenan, H. Yu, M. Siewny, and T. Perkins, J. Chem. Phys. **148**, 123313 (2018).
[10] S. Tafoya, S. Large, S. Liu, C. Bustamante, and D. Sivak, Proc. Natl. Acad. Sci. USA **116**, 5920 (2019).
[11] M. Ribezzi-Crivellari and F. Ritort, Nat. Phys. **15**, 660 (2019).
[12] D. Ross, E. Strychalski, C. Jarzynski, and S. Stavis, Nat. Phys. **14**, 842 (2018).
[13] C. Jarzynski, Phys. Rev. Lett. **78**, 2690 (1997).
[14] G. E. Crooks, Phys. Rev. E **60**, 2721 (1999).
[15] T. Sagawa and M. Ueda, Phys. Rev. Lett. **104**, 090602 (2010).
[16] J. M. R. Parrondo, J. M. Horowitz, and T. Sagawa, Nat. Phys. **11**, 131 (2015).
[17] C. Jarzynski, C. R. Phys. **8**, 495 (2007).
[18] J. Mathé, H. Visram, V. Viasnoff, Y. Rabin, and A. Meller, Biophys. J. **87**, 3205 (2004).
[19] H. Callen, *Thermodynamics and an Introduction to Thermostatistics*, 2nd ed. (Wiley, New York, 1985).
[20] R. Tsukanov, T. E. Tomov, R. Masoud, H. Drory, N. Plavner, M. Liber, and E. Nir, J. Phys. Chem. B **117**, 11932 (2013).
[21] O. Dudko, J. Mathé, A. Szabo, A. Meller, and G. Hummer, Biophys. J. **92**, 4188 (2007).
[22] O. K. Dudko, G. Hummer, and A. Szabo, Proc. Natl. Acad. Sci. USA **105**, 15755 (2008).
[23] J. Horowitz and C. Jarzynski, J. Stat. Mech. (2007) P11002.
[24] G. N. Bochkov and Y. E. Kuzovlev, Phys.-Usp. **56**, 590 (2013).
[25] J. B. Heng, A. Aksimentiev, C. Ho, P. Marks, Y. V. Grinkova, S. Sligar, K. Schulten, and G. Timp, Nano Lett. **5**, 1883 (2005).
[26] Y.-L. Ying and Y.-T. Long, J. Am. Chem. Soc. **141**, 15720 (2019).
[27] A. Laszlo, I. Derrington, and J. Gundlach, Methods **105**, 75 (2016).
[28] A. F. Sauer-Budge, J. A. Nyamwanda, D. K. Lubensky, and D. Branton, Phys. Rev. Lett. **90**, 238101 (2003).
[29] W. Vercoutere, S. Winters-Hilt, H. Olsen, D. Deamer, D. Haussler, and M. Akeson, Nat. Biotechnol. **19**, 248 (2001).
[30] K. Sekimoto and S. Sasa, J. Phys. Soc. Jpn. **66**, 3326 (1997).
[31] M. Gavrilov and J. Bechhoefer, Philos. Trans. R. Soc. A **375**, 20160217 (2017).
[32] F. Douarche, S. Ciliberto, A. Petrosyan, and I. Rabbiosi, Europhys. Lett. **70**, 593 (2005).
[33] A. Pohorille, C. Jarzynski, and C. Chipot, J. Phys. Chem. B **114**, 10235 (2010).
[34] J. Gore, F. Ritort, and C. Bustamante, Proc. Natl. Acad. Sci. USA **100**, 12564 (2003).
[35] M. Palassini and F. Ritort, Phys. Rev. Lett. **107**, 060601 (2011).
[36] K. D. Whitley, M. J. Comstock, and Y. R. Chemla, in *Optical Tweezers: Methods and Protocols*, edited by A. Gennerich (Springer New York, New York, 2017), pp. 183–256.
[37] Y. Jun and J. Bechhoefer, Phys. Rev. E **86**, 061106 (2012).
[38] M. Gavrilov and J. Bechhoefer, Europhys. Lett. **114**, 50002 (2016).
[39] M. Gavrilov and J. Bechhoefer, Phys. Rev. Lett. **117**, 200601 (2016).
[40] M. Gavrilov, R. Chétrite, and J. Bechhoefer, Proc. Natl. Acad. Sci. USA **114**, 11097 (2017).
[41] G. M. Wang, E. M. Sevick, E. Mittag, D. J. Searles, and D. J. Evans, Phys. Rev. Lett. **89**, 050601 (2002).
[42] S. Toyabe, T. Sagawa, M. Ueda, E. Muneyuki, and M. Sano, Nat. Phys. **6**, 988 (2010).
[43] V. Blickle and C. Bechinger, Nat. Phys. **8**, 143 (2012).
[44] A. Bérut, A. Petrosyan, and S. Ciliberto, Europhys. Lett. **103**, 60002 (2013).
[45] J. V. Koski, V. F. Maisi, J. P. Pekola, and D. V. Averin, Proc. Natl. Acad. Sci. USA **111**, 13786 (2014).

[46] I. A. Martínez, É. Roldán, L. Dinis, D. Petrov, J. M. R. Parrondo, and R. A. Rica, Nat. Phys. **12**, 67 (2016).
[47] J. Roßnagel, S. T. Dawkins, K. N. Tolazzi, O. Abah, E. Lutz, F. Schmidt-Kaler, and K. Singer, Science **352**, 325 (2016).
[48] R. W. Friddle, Phys. Rev. Lett. **100**, 019801 (2008).
[49] M. Zuker, Nucl. Acids Res. **31**, 3406 (2003).
[50] J. SantaLucia, Jr., and D. Hicks, Annu. Rev. Biophys. Biomol. Struct. **33**, 415 (2004).
[51] M. Ageno, E. Dore, and C. Frontali, Biophys. J. **9**, 1281 (1969).
[52] M. C. Williams, J. R. Wenner, I. Rouzina, and V. A. Bloomfield, Biophys. J. **80**, 874 (2001).
[53] X. Wang, H. J. Lim, and A. Son, Environ. Anal. Health Toxicol. **29**, e2014007 (2014).
[54] B. A. Berg and R. C. Harris, Comput. Phys. Commun. **179**, 443 (2008).
[55] M. Gavrilov, J. Y. C. Yang, R. S. Zou, W. Ma, C.-Y. Lee, S. Mohapatra, J. Kang, T.-W. Liao, S. Myong, and T. Ha, Nat. Commun. **13**, 6312 (2022).